PROCEEDINGS

4th Osaka University-JWRI/NTU-MSE Workshop

7th March 2019

大阪大学
OSAKA UNIVERSITY

We are now welding

Department of Materials Science and Engineering, National Taiwan University

And

Joining and Welding Research Institute, Osaka University

Content

Accommodation

Just Sleep Taipei NTU (捷絲旅台大會館)

Address: No. 83, Sec. 4, Roosevelt Road, Taipei, 10673, Taiwan
TEL: +886 2 7735 5088

Howard Civil Service International House (福華文教會館)

Address: No. 30, Sec. 3, Sinsheng S. Road, Taipei, Taiwan
TEL: +886 2 7712 2323

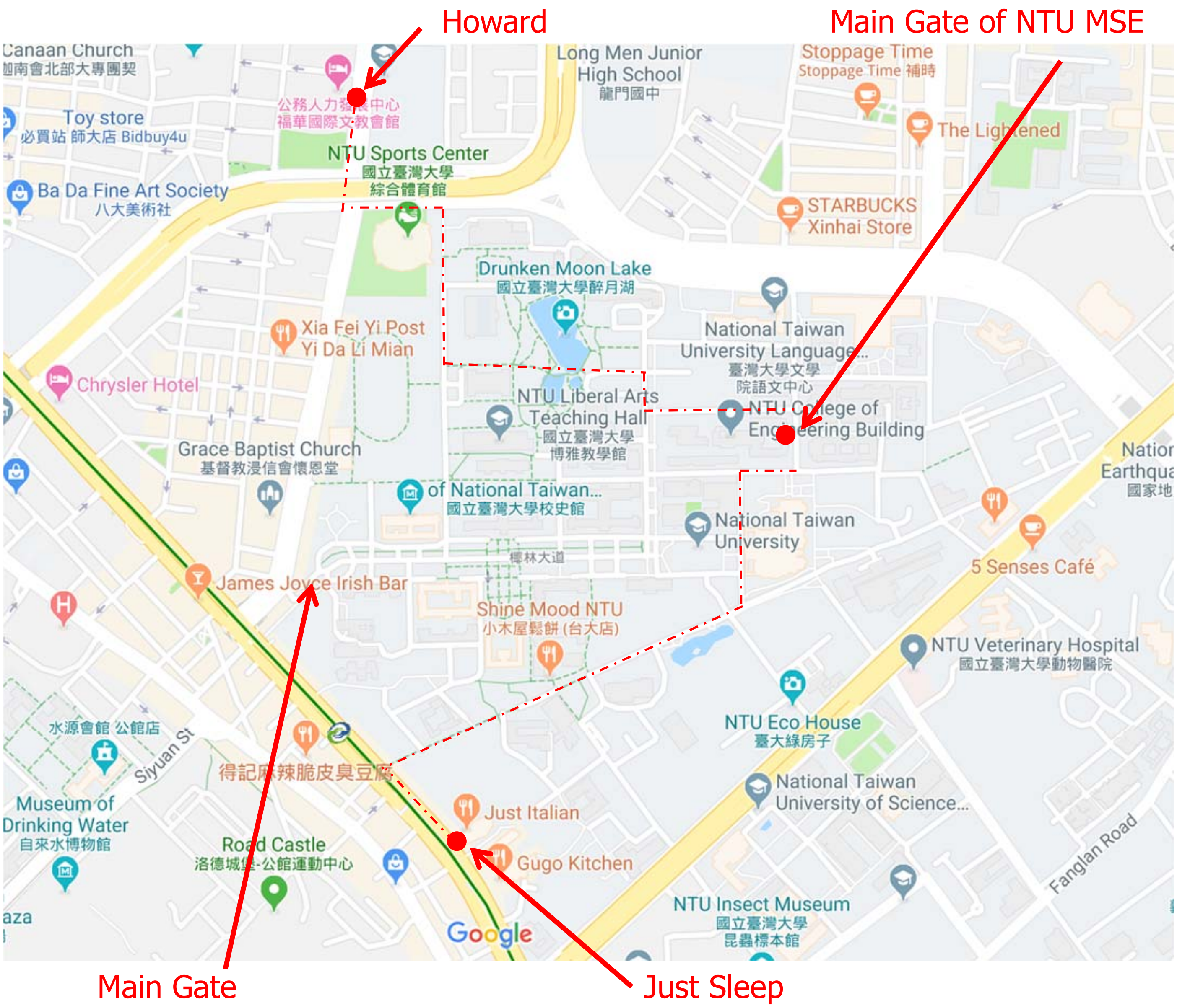

Notification:
Two students will guide you from hotel lobby to NTU MSE at 8:30 AM.

Morning Schedule

Progress in Joining and Interface Science and Technology			
8:30-9:00	**Movement and Registration**		
9:00-9:10	Opening Remarks	NTU-Engineering College NTU-MSE JWRI	Prof. Wen-Chang Chen Prof. Hsin-Chih Lin Prof. Katsuyoshi Kondoh
9:10-9:20	Introducing NTU-MSE	NTU-MSE	Prof. Homer Yen
9:20-9:30	Introducing Osaka U. JWRI	JWRI	Prof. Katsuyoshi Kondoh
9:30-9:50	Strengthening calcium sulfate through microstructural design	NTU-MSE	Prof. Wei-Hsing Tuan
9:50-10:10	Mezzo- and Macro-scale Cyclic Plasticity Analysis for Predicting Seismic Performance and Fatigue Life of Weld Structures	JWRI	Prof. Seiichiro Tsutsumi
10:10-10:30	Low-temperature and Pressureless Cu-to-Cu Bonding by Microfluidic Electroless Interconnection Process	NTU-MSE	Prof. C. Robert Kao
10:30-11:00	**Tea Break and Group Photo Session**		
11:00-11:20	Tribological Property and Biocompatibility of Titanium Plate Coated with Carbon Nanotubes	JWRI	Prof. Junko Umeda
11:20-11:40	Massive ferrite transformation in an interstitial-free steel	NTU-MSE	Prof. Jer-Ren Yang
11:40-12:00	Modeling of Multi-pass Welding, Specimen Machining, Residual Stress Treatment, and Bending Test of Thick-section Welds	JWRI	Prof. Yoshiki Mikami
12:00-13:00	**Lunch Break**		

Afternoon Schedule

Progress in Joining and Interface Science and Technology			
13:00-14:00	**Poster Mini-Presentation**		
14:00-14:20	Atomic layer annealing for atomic layer epitaxy of GaN and AlN thin films at a low growth temperature	NTU-MSE	Prof. Miin-Jang Chen
14:20-14:40	Interface Joining Mechanism of Friction Stir Welding Investigated by Cu/Cu10Zn Interfacial Observation	JWRI	Prof. HuiHong Liu
14:40-15:00	Measuring Hydrogen Escaping from Enameled Steels	NTU-MSE	Prof. Homer Yen
15:00-15:20	Microstructural Control of Austenitic Stainless Steels based on Grain Boundary Engineering	JWRI	Prof. Shun Tokita
15:20-16:00	**Tea Break/Poster Discussion**		
16:00-16:20	**Collaboration Discussion/Department Tour**		
16:20-16:30	**Closing Remarks** Prof. Hsin-Chih Lin & Prof. Katsuyoshi Kondoh		
16:30-17:30	**Hotel Break**		
18:00-20:00	**Banquet**		

1. Primary presentation is 20 min (17 min talk + 3 min Q&A). Please check your slides during breaks.

2. All posters must be ready during the tea break in the morning.

3. All poster authors need to give 3 min mini-presentation. Please provide 1-page slide and send to homeryen@ntu.edu.tw before the session.

4. The style of collaboration discussion is free. Please feel happy to find new collaborators during the workshop.

5. We will meet in hotel lobby at 17:30 and go to the restaurant.

Strengthening calcium sulfate through microstructural design

W. H. Tuan[1]*, H. Y. Chang[1], Y. C. Chen[1], P.Y. Hsu[1], T. Kozwaw[2], A. Kondo[2], M. Naito[2]

[1] Department of Materials Science and Engineering, National Taiwan Unibversity, Taipei, Taiwan
[2] Joint and Welding Research Institute (JWRI), Osaka University, Osaka, Japan

* Corresponding author. E-mail: tuan@ntu.edu.tw

Keywords: bioceramic; calcium sulfate; strength; microstructure

Biocerammics can be generally divided into two groups: biodegradable and non- biodegradable, in terms of their degradation ability in body fluid. One of the biodegradable ceramics is calcium sulfate. This ceramic is superior in its bio-compatibility [1]. Nevertheless, the strength of calcium sulfate is extremely low. One of the reasons for low strength can be related to the exaggerated grain growth during sintering. In the present study, a methodology of microstructure design is adopted to improve the strength of calcium sulfate. A very small amount of fume silica is added into calcium sulfate powder. The particle size ratio for calcium sulfate to fume silica is larger than one order of magnitude. The microstructure of the sintered specimen is then characterized. The silica particles tend to locate at the grain boundaries of calcium sulfate. The growth of calcium sulfate grains is thus prohibited. An amount of silica as low as only 0.5 wt% is capable to double the strength of sintered calcium sulfate.

References

[1] Man-Ping Chang, Hsiu-Ching Hsu, Wei-Hsing Tuan, Po-Liang Lai, Journal of Medical and Biological Engineering, 37, 879-886 (2017).

Mezzo- and Macro-scale Cyclic Plasticity Analysis for Predicting Seismic Performance and Fatigue Life of Weld Structures

Seiichiro Tsutsumi *, Riccardo Fincato, Ramy Gadallah

Joining and Welding Research Institute (JWRI), Osaka University, Osaka, Japan

* Corresponding author. E-mail: tsutsumi@jwri.osaka-u.ac.jp

Keywords: cyclic plasticity, fatigue crack, crystal plasticity, seismic performance, weld structure

Fatigue initiation as a series of damage accumulation and crack initiation is one of the most challenging issues among the fatigue failure processes of materials and structures. Experimental evidence elucidated that the crack initiation is mainly subjected to the damage accumulation which has multi-scale aspects taking the form of macroscopic/microscopic cyclic plasticity represented by such as hysteresis loop, ratcheting and cyclic creep [1-6]. The yield stresses of steels are often prescribed by the experimental stress-strain curves under monotonic loading conditions exhibiting the linear elastic, the upper/lower yielding, the plateau and the hardening responses. The linear/elastic response under a certain lower-stress level than the dominant yielding stress is widely observed not only under monotonic but also under cyclic loading conditions up to a certain number of cycles, so-called macroscopically elastic stress state, in which plastic strain is not observed macroscopically. However, the fatigue failure of steels could be apparently induced, even if all stress amplitudes never exceeded the macroscopic yield stress. Some elaborated fatigue experiment, focused on the damage accumulation under macroscopically elastic condition, has revealed that the plastic stain is suddenly generated after a certain number of cycles. To understand and evaluate the fatigue processes of materials, the unconventional plasticity model and the crystal plasticity FE analyses model are proposed by the authors for the description of the cyclic loading behavior of metals not only under macroscopic yielding but also under macroscopically elastic condition. In this study, the multi-scale aspects of fatigue problems are examined by the cyclic plasticity modeling and the crystal plasticity FE analyses.

References

[1] S. Tsutsumi and R. Fincato, Materials and Design, 165, 107573, (2019).
[2] R. Fincato, S.Tsutsumi, H. Momii, Fracture and Structural Integrity, 47, 231-246, (2019).
[3] S. Tsutsumi, K. Ueda, R. Fincato, J. of Structural Engineering, JSCE, 64A, 627-635, (2018).
[4] R. Fincato and S.Tsutsumi, Int. J. Solids and Structures, Available online, (2018).
[5] R. Gadallah, N. Osawa, S. Tanaka, S. Tsutsumi, Engineering Fracture Mechanics, 197(5) 48-65, (2018).

Low-Temperature and Pressureless Cu-to-Cu Bonding By Microfluidic Electroless Interconnection Process

C. Robert Kao *

Department of Materials Science and Engineering, National Taiwan University, Taipei, Taiwan

* Corresponding author. E-mail: crkao@ntu.edu.tw

Keywords: Electroless plating, Low temperature bonding, Pressureless bonding;

Increasing demands for high-performance miniaturized electronic devices have driven the semiconductor industry toward finer pitch and higher interconnect density. Thermocompression bonding, with the necessity of applying force and heat, is now being adopted for high-density interconnections. However, there are many challenges that needed to be conquered, such as warpage-induced defects, cracking of delicate chips and thermal drift. To address these issues, a novel Cu-to-Cu bonding process called microfluidic electroless interconnection has been developed. The electroless plating process was conducted under controlled flow in an airtight microfluidic fixture. The bonding temperature can be lower than 80 °C, which is an ideal condition for bonding. The bonded pillars were analyzed by scanning electron microscope and electron probe micro-analyzer. Besides, to further confirm and to avoid the damage created by polishing steps, a focused ion beam was also used for the observation. This innovative low-temperature, pressureless electroless bonding approach shows considerable promise for applications that require low stress and low thermal budget process.

Tribological Property and Biocompatibility of Titanium Plate Coated with Carbon Nanotubes

J. Umeda[1]*, K. Kondoh[1], E. Nishida[2], H. Miyaji[2], B. Fugetsu[3]

[1] Joining and Welding Research Institute, (JWRI), Osaka University, Osaka, Japan
[2] Graduate School of Dental Medicine, Hokkaido University, Japan
[3] Policy Alternatives Research Institute, The University of Tokyo, Japan

* Corresponding author. E-mail: umedaj@jwri.osaka-u.ac.jp

Keywords: Carbon nanotubes (CNTs), Titanium, Tribological property, Biocompatibility

CNTs are possessed of attractive additives to materials for tribological [1] and biomedical applications [2]. Titanium is also widely used as a structural material in various industrial components and in dental implants [3] because of its low density, superior mechanical properties and good corrosion resistance. On the other hand, Titanium and its alloy have poor tribological properties when in contact with other materials and itself [4]. Thus, it is expected titanium composites coatings with carbon nanotubes would have excellent tribological property and biocompatibility.

In this study, the individually independent MWCNTs were uniformly dispersed in isopropyl alcohol based zwitterionic surfactant solution, which was effective to obstruct oxidation of metal substrate in contact with CNTs solution. Ti plate was dipped into the solution, and subsequently served to heat treatment at 973~1253 K by using vacuum furnace. Microstructure and phase characterization were investigated by X-ray diffraction (XRD), and by optical and scanning electron microscopy (SEM) equipped with EDS analyzer. Network-structured MWCNTs were coated on Ti plate surface. In addition, in-situ synthesis of titanium carbides (TiC) by the reaction of Ti plate and CNTs occurred in heat treatment, and these carbides were detected by XRD and SEM-EDS. Vicker's micro-hardness near the interface between Ti plate surface and coated CNT films was remarkably higher than that of inside Ti plate. This was because carbon solid solution originated from CNT films occurred during heat treatment, and resulted in hardening of Ti plate.

For evaluating the tribological properiy, Ti coated with un-bundled MWCNTs was examined by the ball-on–disk wear test equipment under dry conditions at ambient temperature. SUS304 stainless steel ball was used as the counter material. The mean friction coefficient of the Ti plate coated with MWCNTs was 0.19, and significantly lower and stable compared to pure Ti plate without any coating, showing 1.09 friction coefficient and some seizure areas. SEM-EDS observation on the wear tracks of the plate indicated that network-structured MWCNT films obviously remained even after 3.6 ks in sliding. These results were due to no adhesion and stick-slip phenomenon on Ti plate surface coated with CNT films in contacting with the SUS304 ball. These superior tribological performances were caused by the defensive by hard TiC dispersions, Ti plate hardening by carbon solid solution, and self-lubricant effect by network-structured MWCNTs coated on Ti plate surface.

In order to investigate the biocompatibility, the cell culture test was conducted on the Ti plate coated with MWCNTs. Cell spreading and proliferation on the Ti plate were promoted by MWCNTs. In addition, bone morphogenetic protein was placed on the rat cranial bone and histological analysis was carried out. MWCNTs onto Ti plate showed good tissue-compatibility and new bone formation in rat implantation.

This study certainly prospects the possibility of improving tribological properties and biocompability for titanium composites coatings with carbon nanotubes .

References

[1] J. Umeda, B. Fugetsu, E. Nishida, H. Miyaji, K. Kondoh, Appl. Surf. Sci. 357 (2015) 721-727.
[2] RK Sinha, RS Tuan, Bone 18 (1996) 451-457.
[3] K.G. Budinski, Wear 151 (1991) 203-217.
[4] Y. Usui, K. Aoki, N. Narita, etc., Small 4 (2008) 240-246.

Massive ferrite transformation in an interstitial-free steel

P. H. Liu and J. R. Yang*

Department of Materials Science and Engineering, National Taiwan University, Taipei, Taiwan

* Corresponding author. E-mail: jryang@ntu.edu.tw

Keywords: Interstitial-Free Steel; Massive ferrite; Continuous cooling transformation; Dilatometer; Transmission Electron Microscopy (TEM)

To develop very lean alloying steels with excellent formability and weldability, the interstitial-free (IF) steels have been widely applied in industry. These steels have a low yield strength, a high plastic strain ratio (r-value) and a high strain rate sensitivity. Nowadays, IF steels are widely known as the superior material for deep drawing operations. They have been utilized for broad applications ranging from automotive bodies to electronic components as well as house hold appliances. The occurrence of the massive ferrite transformation in heat treated or welded IF steels is an intriguing subject and worth further research. However, in the past five decades, just a few works have investigated in this subject (probably due to the precision limit of the cooling rate for experiment), and the corresponding microstructural characterizations have focused mostly on optical metallography. The detailed microstructural characterization of massive ferrite in IF steels is in need of further investigation.

A massive ferrite formation in an interstitial-free (IF) steel with three different austenitization conditions (at 1200, 1100 and 1000°C respectively for 3 min) was investigated. To conduct the rapid continuous-cooling transformations with a cooling rate of 500°C/s, hollow rod specimens were employed in a dilatometer. Thermal arrests, which were associated with the phase transition, were detected in the cooling curves, and thereby the massive ferrite transformation temperatures were determined. The corresponding treated samples were studied by optical metallography and transmission electron microscopy (TEM). The features of massive ferrite (Fig. 1) and its transformation characterization are discussed.

References

[1] H.K.D.H. Bhadeshia, R.W.K. Honeycombe, Steels: microstructure and properties, 4th edition, 2017.

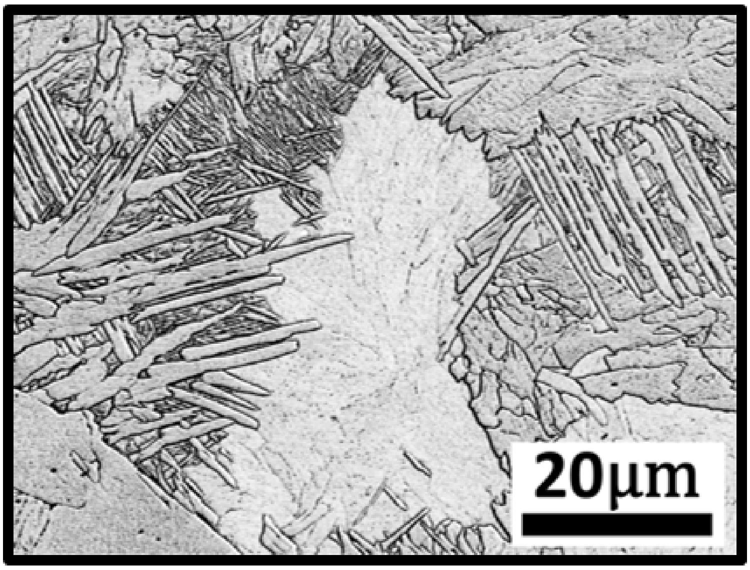

Fig.1 Optical micrograph displays massive ferrite, Widmanstätten ferrite, bainite and Martensite.

Modeling of Multi-pass Welding, Specimen Machining, Residual Stress Treatment, and Bending Test of Thick-section Welds

Y. Mikami[1]*, T. Kawabata[2]

[1] Joining and Welding Research Institute (JWRI), Osaka University, Osaka, Japan
[2] Graduate School of Engineering, The University of Tokyo, Tokyo, Japan

* Corresponding author. E-mail: mikami@jwri.osaka-u.ac.jp

Keywords: multipass welds, residual stress modification, fracture toughness test, crack-tip opening displacement

Weld residual stress occurs inevitably in weld joints and it affects the joint performance such as fracture toughness, fatigue life, and buckling strength, etc. Therefore, the consideration of the weld residual stress is important in the design and evaluation of the integrity of weld joints. The effect of weld residual stress has usually been considered by increasing applied stress; however, more detaild consideration is required to refine and rationalize the design and evaluation procedure.

In this study, a numerical simulation model was developed to incorporate the weld residual stress in bending tests of welded joints. Firstly, multi-pass welding was simulated to calculate the residual stress distribution of the weld joints. Secondly, machining process for extracting a bend specimen was modeled to simulate the redistribution of the residual stress. Finally, bending load was applied to the specimen. In addition, residual stress modification was also modeled to investigate the variation of the residual stress distribution and its influence on the bending test results.

Consequently, the test result varied depending on the consideration of the weld residual stress. Threfore, it is important to incorporate the effect of the weld residual stress more in detail in the design and evaluation process of weld joints.

References

[1] Y. Mikami, et al., Theor. Appl. Fract. Mech., 92, 214–222 (2017).
[2] Y. Mikami, et al., Proc. Struct. Integ., 13, 1804–1810 (2018).

Atomic layer annealing for atomic layer epitaxy of GaN and AlN thin films at a low growth temperature

Wei-Hao Lee, Wei-Chung Kao, and Miin-Jang Chen*

Department of Materials Science and Engineering, National Taiwan University, Taipei, Taiwan

* Corresponding author. E-mail: mjchen@ntu.edu.tw

Keywords: Atomic layer deposition, atomic layer epitaxy, atomic layer annealing, GaN, AlN

Atomic layer deposition (ALD) is an attractive technique for preparing high-quality nanoscale thin films, and has been widely exploited in a great variety of nanoscale applications including solar cells, memories, and transistors. However, as-deposited thin films prepared by ALD are generally of amorphous-like structure due to the requirement of a low deposition temperature to keep self-limiting chemical reactions in ALD. As compared with amorphous films, crystalline films or even single-crystalline epitaxial layers are more favored because of significantly improved optical and electrical properties. Therefore, it is highly demanded to improve crystallization of ALD-deposited thin films. In this work, a novel concept and approach termed as "atomic layer annealing" (ALA) was proposed in the ALD process to realize the low-temperature atomic layer epitaxy, i.e., to achieve high-quality epitaxial growth of GaN and AlN at a low deposition temperature of only 300ºC on sapphire substrate. Rather than a high growth temperature which is needed in conventional epitaxial growth techniques, a layer-by-layer, in-situ plasma treatment was introduced into each ALD cycle to realize the ALA effect. The plasma treatment during each ALD cycle provides sufficient crystallization energy to the surface of thin films from the incident radicals or ions, leading to the dramatic transformation of the GaN and AlN thin films from the amorphous phase to a single-crystalline epitaxial layer. The X-ray diffraction and high-resolution transmission electron microscopy clearly indicates a high-quality single-crystal GaN and AlN epilayer with only a few tens of nanometer in thickness. The result demonstrates great potential for further extension of the ALD tools from the conventional deposition of amorphous thin films to high-quality epitaxial growth at a low temperature, which can be utilized in a variety of fields and applications in the near future.

Interface Joining Mechanism of Friction Stir Welding Investigated by Cu/Cu10Zn Interfacial Observation

Huihong Liu[1]*, Kohsaku Ushioda[1], Hidetoshi Fujii[1]

[1] Joining and Welding Research Institute (JWRI), Osaka University, Osaka, Japan

* Corresponding author. E-mail: liuhh@jwri.osaka-u.ac.jp

Keywords: Friction stir welding, Microstructure, Interface joining mechanism

Friction stir welding (FSW) is an innovative joining technique which was developed in 1991 [1]. Since FSW enables the solid state joining which effectively avoids the fusion-welding-associated-issues, it has been extensively applied in low-melting-point materials and also expanded to many high-melting-point materials. So far, most of the FSW researchers have made great efforts on clarifying the relationship between welding parameters, microstructure and mechanical properties of the weld joints aiming to fabricate the sound FSW joints [2]. Moreover, heat transfer, strain and strain rate and material flow during FSW were also extensively investigated in order to fully understand the physical fundamentals of FSW [3-5]. However, how the initially unbonded interface of the work-pieces is joined during FSW is still out of understanding even though it is the most fundamental principle of FSW. In this study, a butt FSW was performed on Cu and Cu-10Zn alloy plates. The microstructural evolution along the Cu/Cu-10Zn interface was systematically investigated in order to elucidate the interface joining mechanism of FSW.

Cu and Cu-10Zn alloy plates were subjected to a butt FSW. The probe-extraction-site TD (transverse direction)-WD (welding direction) surface specimen was prepared from the obtained FSW joint and then examined by an optical microscope (Fig. 1) [6]. It is seen that the Cu/Cu-10Zn interface is clearly retained and visible after FSW. In the following, thin film specimens were prepared at various positions along the visible Cu/Cu-10Zn interface by focused ion beam (FIB) and then subjected to a microstructural analysis by TEM.

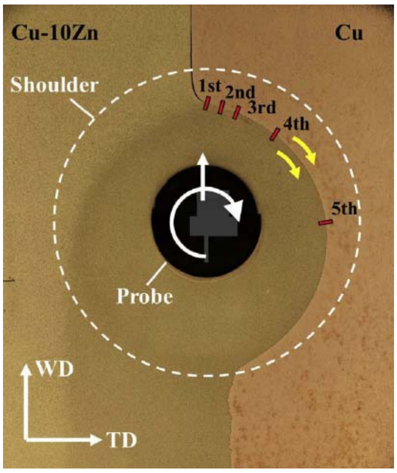

Fig. 1. Optical micrograph of the probe-extraction-site TD-WD surface specimen and thin foil specimen preparation [6].

Based on the obtained results, the interface joining mechanism of FSW is inferred as follows. The initial interface of work-pieces is completely unbonded with lots of large oxides dispersed on the interface. The large oxides are then fragmented into small particles, and the oxide layer is ruptured by the shear force, compressive force and interface material deformation, which produces fresh surfaces on both Cu and Cu-10Zn sides. These fresh surfaces are thus atomically joined under the compressive force, while leaving the small oxide particles still distributed on the interface with a void formation besides the particles. A strain-induced grain boundary migration driven by the stored energy difference between opposite sides of the grain boundary will occur on the interface, assisting to extinguish the voids around the oxide particles. Finally, a sound interface joining without oxide particles and voids remaining on the interface can be obtained during FSW.

References

[1] W.M. Thomas, et al., G.B. Patent Application No. 9125978.8, 1991.
[2] Y.F. Sun, H. Fujii, Mater. Sci. Eng. A, 527, 6879-6886 (2010).
[3] R. Nandan, G.G. Roy, T. Debroy, Metall. Mater. Trans. A, 37, 1247-1259 (2006).
[4] A. Arora, Z. Zhang, A. De, T. DebRoy, Scripta Mater., 61, 863-866 (2009).
[5] Y. Morisada, H. Fujii, Y. Kawahito, K. Nakata, M. Tanaka, Scripta Mater., 65, 1085-1088 (2011).
[6] H.H. Liu, K. Ushioda, H. Fujii, Acta Mater., 166, 324-334 (2019).

Measuring Hydrogen Escaping from Enameled Steels

Yi-Ting Lin[1], Yu-Chen Lin[1], Lung-Jen Chiang[2], Hung-Wei (Homer) Yen[1]*

[1] Department of Materials Science and Engineering, National Taiwan University, Taipei, Taiwan
[2] Department of R&D of Iron and Steel, China Steel Corporation, Kaohsiung, Taiwan

* Corresponding author. E-mail: homeryen@ntu.edu.tw

Keywords: Hydrogen; Thermal Desorption Analysis; Fishscale; Enameled Steel

Enameling is a process that fuses a layer of glass onto metal objects in order to enhance surface properties and beauty. In this process, nascent hydrogen diffuses from enamel into base metal during firing, and, during cooling, hydrogen tends to escape out due to decreasing solubility of hydrogen in steel. Hence, if hydrogen cannot be effectively trapped, spontaneous popping-up of enamel chips will occur. This is called fishscaling as seen in Fig. 1 [1]. The design of steels for enameling is confronted with controlling trapping sites for hydrogen. Moreover, measurements evaluating capability of hydrogen trapping in steel must be crucial in this field.

Permeation test (PT) and thermal desorption analysis (TDA) have long been applied to evaluate capability of hydrogen trapping in steels [2]. Although some correlations had been investigated for enameled steels, many contradictions still cannot be explained based on these two methods. The current presentation will start from some of these contradictions in enameled steels. Moreover, we will demonstrate more comprehensive experiments to clarify relationship between hydrogen and trapping sites especially for enameled steels. In this study, it is found that hydrogen trapped by fractal titanium nitrides is non-diffusible. These hydrogen solutes/molecules become diffusible when they are just beneath surface of steel. Moreover, interface between enamel and steel is effective trapping site, and its capability can be affected by microstructure of steel. All these outcomes can be applied to design new steel for enameling.

The current research will assist the development of measuring methods of hydrogen trapping for enameled steel. It also enables ideas in designing new enameled steels by controlling proper trapping sites and trapping mechanisms.

References

[1] E.I. Litvinova. Causes of fish scaling on steel enamels, Glass and Ceramics 35 (1978) 533-537.
[2] H. Bhadeshia. Prevention of Hydrogen Embrittlement in Steels, ISIJ International 56 (2016) 24-36.

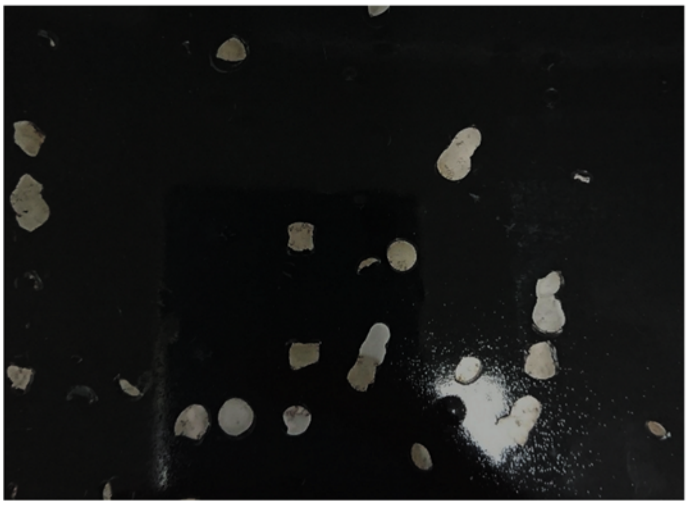

Fig. 1 Fishscaling on the surface of enameled steel.

Microstructural Control of Austenitic Stainless Steels based on Grain Boundary Engineering

S. Tokita*, K. Kadoi, H. Inoue

Joining and Welding Research Institute (JWRI), Osaka University, Osaka, Japan

* Corresponding author. E-mail: tokita@jwri.osaka-u.ac.jp

Keywords: Stainless steel, EBSD, Intergranular corrosion, Grain boundary engineering

Austenitic stainless steels have been widely used in many industrial applications due to their good mechanical properties and corrosion resistance. However, degradation of materials properties such as corrosion and cracking during welding process has been a severe problem. Fundamental researches have shown that the properties of metal materials often depend on the structure, character and distribution of grain boundaries, namely grain boundary character distribution (GBCD). Coincident site lattice boundaries (CSL boundaries) tend to have higher resistance to grain boundary degradations than the other random boundaries. The previous study has shown that the intergranular corrosion resistance was improved by increasing the length ratio of CSL boundaries through the thermomechanical process. However, further understanding of microstructure evolution mechanism during the thermomechanical process is required for optimization of process and process reliability. Therefore, the objective of this study is to investigate the microstructure evolution mechanism during grain boundary engineering process by systematic experiments of thermomechanical process parameters.

Type 304 and 310 austenitic stainless steels were used in this study. As received material was solution heat treated in 1050 to 1100 °C and quenched in cold water. A thermomechanical process which consists with cold rolling and annealing was performed to increase the length ratio of CSL boundaries. Electron backscatter diffraction (EBSD) analysis was conducted to analyze the GBCD of the specimens. Intergranular corrosion resistance of specimens was measured by ferric sulfate-sulfuric acid corrosion test.

The GBCD of thermomechanical processed materials was mainly affected by the reduction ratio of cold rolling. The 3% cold rolled and annealed specimen showed a drastic increase of length ratio of CSL boundaries. In-situ EBSD analysis has shown that the optimization of GBCD was achieved by abnormal grain growth and annealing twining. Specimens with a higher ratio of CSL boundaries tend to show higher intergranular corrosion resistance. Adequate improvement of intergranular corrosion resistance required longer annealing time, rather than an increase of CSL boundaries. It is considered that the reduction of residual strain by long-time annealing was required for the steady improvement of intergranular corrosion resistance.

[P01] Synchrotron X-ray Nanoprobe Study of Sn Whisker Growth

Pei-Tzu Lee[1, *], Cheng-Yu Lee[2], Wan-Zhen Hsieh[3], Mau-Tsu Tang[3], Shao-Chin Tseng[3], C. Robert Kao[1]

[1] Department of Materials Science & Engineering, National Taiwan University, Taipei, Taiwan
[2] Department of Chemical Engineering & Materials Science, Yuan Ze University, Taoyuan, Taiwan
[3] National Synchrotron Radiation Research Center (NSRRC), Hsinchu, Taiwan

* Corresponding author. E-mail: patslee1994@gmail.com

Keywords: Synchrotron Radiation, X-ray fluorescence, Electromigration, Sn Whiskers

Tin (Sn) whiskers have become a serious reliability concern in recent years because of the utilization of lead (Pb)-free solders and surface finishes in commercial electronics. In this study, we conducted an analysis via synchrotron X-ray nanoprobe optics (beamline 23A, Taiwan Photon Source) to characterize the Sn electromigration and the Sn whisker growth behavior upon electron current stressing. X-ray fluorescence mapping (XFM) offers elemental detection with a resolution down to the tens of nm. X-ray fluorescence was monitored to quantify the evolution of the Sn surface morphology and the formation of Sn whiskers/extrusions with increasing current stressing time (t). These characterizations will not only advance our own knowledge of Sn whiskering mechanism, but be helpful in development of the microelectronic surface finishing technology.

[P02] Study of Sn-45Bi-2.6Zn alloy with low-melting temperature and improved elongation

Shiqi Zhou[1,2]*, Chih-han Yang[3], Yu-An Shen[1], Shih-kang Lin[3,4,5], and Hiroshi Nishikawa[1]

[1] Joining and Welding Research Institute (JWRI), Osaka University, Osaka, Japan
[2] Graduate School of Engineering, Osaka University, Osaka, Japan
[3] Department of Materials Science and Engineering, National Cheng Kung University, Tainan, Taiwan
[4] Hierarchical Green-Energy Materials (Hi-GEM) Research Center, National Cheng Kung University, Tainan, Taiwan
[5] Center for Micro/Nano Science and Technology, National Cheng Kung University, Tainan, Taiwan

[*] Corresponding author. E-mail: charleszhou1992@gmail.com

Keywords: Sn-58Bi, low-temperature alloy, ductility, off-eutectic, thermaldynamic calculation

It has always been a challenge to develop a low-melting temperature lead-free solder with great mechanical properties and thermal reliability. Recently, eutectic Sn-58 wt. %Bi (Sn58Bi) solder alloy has been considered as a. However, brittleness and microstructural coarsening issues of Sn58Bi alloy have not yet been fundamentally solved. It is noted that the ductility improvements in these alloys are often limited and the ultimate tensile strength (UTS) is usually sacrificed simultaneously. Because Bi with a large volume fraction of 58 wt. % in eutectic Sn-58Bi has always been the main cause of low ductility of the bulk alloy, lowering the Bi volume fraction is considered an ultimate solution.

To replace eutectic Sn58Bi alloy, the newly designed alloy with good wettability is required, in other words, melting temperature should be comparable with eutectic Sn58Bi and mushy temperature zone should be as narrow as possible. In this study, the composition of 51Sn-46.3Bi-2.7Zn was designed to achieve aforementioned two targets, i.e. decreasing Bi to Sn volume fraction and controlling liquidus temperature and mushy zoon.

For alloying process, starting materials were melted in-house at 700 °C for 5 h. Next, the newly produced alloy was subsequently remelted at 250 °C for 1 h to ensure its homogenization. The compositions of the alloys were measured using inductively coupled plasma optical emission spectroscopy (ICP-OES) after the alloying procedure. The precise composition of Sn was found to be 52.34 wt. %, Bi was 45.04 wt. %, and Zn was 2.61 wt. %. Then, a bar-shaped mold was used for casting. Solid-state thermal aging test was performed in an oil bath at 80 °C for 504 and 1008 h. Then, tensile test was conducted after bar-shaped alloys were machined into a dumbbell shape.

Eutectic Sn-58Bi alloy was dominated by a Sn-Bi eutectic mixture, as well as a very small amount of Sn-rich dendrite decorated with Bi precipitates inside. On the other hand, 51Sn-46.3Bi-2.7Zn had significantly higher volume fraction of Sn-rich dendrite than that of eutectic Sn-58Bi. Additionally, a ternary mixture, which consisted of interlocked Bi-rich and Sn-rich with black color Zn dispersed in them was observed. Approximately 112 % elongation improvement was obtained of 51Sn-46.3Bi-2.7Zn alloy compared to that of the eutectic Sn-58Bi alloy, owing to the increased Sn to Bi volume ratio. After thermal aging, the elongation improvement is predicted maintains, probably due to the hindering effect of Zn segregation on the Sn-Bi phase boundary during thermal aging, which was discovered in our previous study [1].

References

[1] Zhou, S. et al. Improvement in the mechanical properties of eutectic Sn58Bi alloy by 0.5 and 1 wt.% Zn addition before and after thermal aging. Journal of Alloys and Compounds (2018).

[P03] Sintering of Strontium-doped Calcium Sulfate bone void filler

Ying-Cen Chen[1*],Wei-Hsing Tuan [1]

[1] Department of Materials Science and Engineering, National Taiwan University, Taiwan

[*] Corresponding author. E-mail: D04527005@ntu.edu.tw

Keywords: calcium sulfate anhydrate, strontium, bioresorbable,

Calcium sulfate ($CaSO_4$, CS) has been used as bone graft substitute for more than 100 years. In addition, there are three forms of calcium sulfate: calcium sulfate dihydrate ($CaSO_4 \cdot 2H_2O$), calcium sulfate hemihydrate ($CaSO_4 \cdot 1/2H_2O$, CSH) and calcium sulfate anhydrate ($CaSO_4$, CSA) in terms of the amount of crystallization water. Calcium sulfate dihydrate and calcium sulfate hemihydrate have been widely used in clinically due to their self-setting and bioresorbable characteristics. A heat treatment can be applied to remove the crystallization water from calcium sulfate dihydrate to form hemihydrate, a subsequent heat treatment can transform produce anhydrate. The hemihydrate can also react with water to form dihydrate.

The rehydratione procedure is also known as self-setting, this reaction is widely used for various clinical applications. More importantly, the calcium sulfate is degradable in water. In the present study, the degradation behavior is tailored through the substition of calcium ions with strontium ions. A sintering technique is used to prepare calcium sulfate anhydrate specimens incorporating strontium ion. The sintering temperature varied from 400°C to 1200°C. In addition, The phase relationships for the strontium-substituted calcium sulfate are then investigated. The density, weight loss, microstructure, strength, cell viability on the specimen are then investigated.

The indirect cytotoxicity results demonstrate that the strontium-substituted calcium sulfate is biocompatibility.

References

[1] W. S. Pietrzak and R. Ronk, "Calcium Sulfate Bone Void Filler: A Review and a Look Ahead," The Journal of Craniofacial Surgery, 11 [4] 327-33 (2000).
[2] J.-L. Wang, Y.-T. Zin, C.-C. Tzeng, C.-I. Lin, S.-W. Lin, and G.-L. Chang, "The Assay of Bone Reaction after Implantation of Calcium Sulfate and a Composite of Calcium Sulfate and Calcium Phosphate," Journal of Medical and Biological Engineering, 23 [4] 205-12 (2003).
[3] W.-J. Chen, T.-T. Tsai, L.-H. Chen, C.-C. Niu, P.-L. Lai, T.-S. Fu, and K. McCarthy, "The Fusion Rate of Calcium Sulfate with Local Autograft Bone Compared with Autologous Iliac Bone Graft for Instrumented Short-Segment Spinal Fusion," Spine, 30 [20] 2293-97 (2005).
[4] F. Wirsching, "Calcium Sulfate," Ullmann's encyclopedia of industrial chemistry (2000).
[5] E. Gentleman, Y. C. Fredholm, G. Jell, N. Lotfibakhshaiesh, M. D. O'Donnell, R. G. Hill, and M. M. Stevens, "The Effects of Strontium-Substituted Bioactive Glasses on Osteoblasts and Osteoclasts in Vitro," Biomaterials, 31 [14] 3949-56 (2010).
[6] R. Suganthi, K. Elayaraja, M. A. Joshy, V. S. Chandra, E. Girija, and S. N. Kalkura, "Fibrous Growth of Strontium Substituted Hydroxyapatite and Its Drug Release," Materials Science Engineering: C, 31 [3] 593-99 (2011).
[7] S. Yuhui99, P. Haobo99, D. BrianW99, L. WilliamW99, and D. Lianfu99, "Effects of Strontium in Modified Biomaterials," Acta Biomaterialia, 7 [2] 800-08 (2011).
[8] I. 10993-5, "Biological Evaluation of Medical Devices–Part 5: Tests for in Vitro Cytotoxicity," Journal[Issue] (2009).
[9] E. ISO, "10993-12, Biological Evaluation of Medical Devices-Part 12, Sample Preparation and Reference Materials," British Standards Institution, UK (2004).
[10] H. Liao, Y. Sun, and G. Sun, "Correlation between Mechanical Properties and Amount of Dendritic A-Al Phase in as-Cast near-Eutectic Al–11.6% Si Alloys Modified with Strontium," Materials Science Engineering: A, 335 [1-2] 62-66 (2002).

[P04] Porous biphasic bone graft substitute prepared by gel-casting

Hao-Yu Chang [1]*, Wei-Hsing Tuan[1*], Po-Liang Lai[2]

[1] Department of Materials Science and Engineering, National Taiwan University, Taipei, Taiwan
[2] Department of Orthopedic Surgery, Chang Gung Memorial Hospital at Linkou, Chang Gung University, College of Medicine, Taoyuan, Taiwan

* Corresponding author. E-mail: d04527002@ntu.edu.tw

Keywords: Bioceramic; Microstructure; Biodegradation

In the present study, hydroxyapatite and calcium sulfate anhydrate has been chosen as biomaterials to produce the porous bone graft substitute through a gel-casting technique. The properties such as biocompatibility and osteoconduction led the hydroxyapatite and calcium sulfate feasible to produce the porous bone graft substitute. The porous composite specimen is mixed with 50 wt% of hydroxyapatite and 50 wt% calcium sulfate in the present study; the resulting porosity is around 69% and the pore size is around 110 μm. The compressive strength of composite specimens is 8.3 MPa, which is higher than that of pure calcium sulfate specimen.

The biodegradation rate of the composite specimen is lower than that of the pure calcium sulfate specimens. After 10 weeks of the degradation test, the weight loss of the composite specimens is around 48%, but the weight loss of the pure calicium sulfate specimens is higher than 90%. The cell viability is evaluated by the MTT assay using MC3T3-E1 cells. The composite specimen is implanted in the Rat's distal femur bone defect for 12 weeks to investigate the new bone formation. The percentage of new bone formation at the orthotopic bone defect after implanting the composite specimen was about 50%, but the percentage of new bone formation in the defect without implant was just 15%, confirming that the composite specimen with hydroxyapatite and calcium sulfate could enhance bone formation.

[P05] Ductility improvement mechanism of pure titanium with oxygen solid solution after water quenching

S. KARIYA[1]*, J. UMEDA[2], K. KONDOH[2]

[1] Department of Mechanical Engineering, Osaka University, Osaka, Japan
[2] Joining and Welding Research Institute (JWRI), Osaka University, Osaka, Japan

* Corresponding author. E-mail: kariya-s@jwri.osaka-u.ac.jp

Keywords: Titanium, Oxygen, Solid solution, Rapid cooling, Ductility improvement

Titanium (Ti) and its alloy have been widely used as excellent structural material in many fields due to their promising properties. Oxygen addition on titanium was restricted while oxygen solid solution have a high hardening effect on Ti and its alloys due to its embrittlement effect. This study clarified the ductility of powder metallurgy (PM) α-titanium (Ti) material with dissolved 0.94 mass% O is improved by water quenching (WQ) at specific temperature, and the effect of WQ on microstructures and tensile properties of Ti-O material was investigated in order to reveal the mechanism of ductility improvement.

The extruded PM Ti rod with uniform oxygen solution, having α-Ti grains with about 10 μm in diameter, was fabricated by using the elemental mixture of pure Ti and TiO_2 powders. Subsequently, the water quenching was applied to the Ti rod after isothermal annealing at 1173~1373 K for 1.8 ks in Ar flow. The microstructures and tensile properties was investigated by SEM-EBSD and EPMA analisys and tensile test.

Tensile test results at the ambient temperature indicated that ultimate tensile strength (UTS) of the specimens after WQ at 1223 K and 1273 K, where Ti-0.94 mass% O material had α+β dual phases, was 993MPa and 988 MPa while that of as-extruded Ti rod without WQ was 1079 MPa. On the other hand, the elongation to failure of the quenched ones at 1223 K and 1273 K was 12.5% and 19.1%, respectively. They are significantly higher than that of as-extruded specimen with 7.5% elongation. The Ti-0.94 mass% O materials with the above WQ treatment consisted of equiaxed grains with about 30 μm in diameter, and some martensite phases were also detected on the grain boundaries. In addition, they had orientation misfits in α-Ti grains, which were formed in α-Ti grain.In the α′-Ti, the {10-11} twin, which is obserced in α′-Ti formed via rapid cooling process from β-Ti[1], was comfirmed. And the EPMA analysisresult (Fig. 1) shows that oxygen content in α-Ti grain was increased to 1.40 mass% and that in α′-Ti and orientation misfit was decreased to 0.56 mass%. According to the binary phase diagram, Ti-0.94 mass% O is consisted of β phase with low oxygen content and α phase with high oxygen content on 1273 K[2]. In these ductile WQed Ti-0.94 mass% O material, it is confirmed that plastic deformation was mainly introduced on these low oxygen area (α′-Ti and orientation misfit) by KAM analisys (Fig. 2). Jaffee's report suggested that the elongation of Ti-0.56 mass% O is over than 15%[3]. These results mean that low oxygen content area originated from β-Ti was ductile enough to take on plastic deformation and elongation was improved to 19.1%.

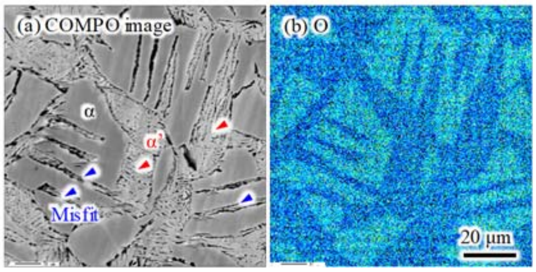

Fig. 1 COMPO image O (a) and distribution map

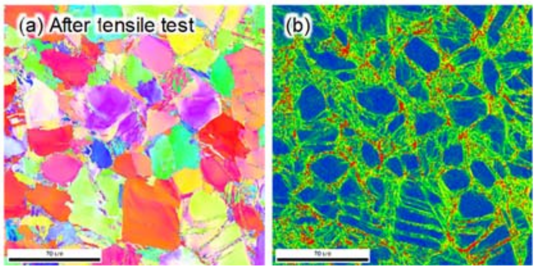

Fig. 2 IPF map (a) and KAM map (b) of WQed Ti-0.94 mass% O afte tensile test.

References
[1] D. A. Porter et. al., Phase Transformations in Metals and Alloys, 2nd ed. London: Chapman & Hall, 1992.
[2] J. L. Murray, "Phase Diagrams of Binary Titanium Alloys," ASM International, Ohio, 1987.
[3] R. I. Jaffee, "The physical metallurgy of titanium alloys," Prog. Met. Phys., vol. 7, pp. 65–163, 1958.

[P06] Precipitation on grain boundaries of the AA7050 (Al-Zn-Mg-Cu) aluminum alloy

Tsai-Fu Chung[1], Yo-Lun Yang[2], Chien-Nan Hsiao[3], Wei-Chih Li[4], Jer-Ren Yang[1,*]

[1] Department of Materials Science and Engineering, National Taiwan University, Taipei, Taiwan
[2] Department of Mechanical Engineering, Imperial College London, London SW7 2AZ, UK
[3] Instrument Technology Research Center, National Applied Research Lab, Hsinchu, Taiwan
[4] E.A. Fischione Instruments, Inc., 9003 Corporate Circle, Export, PA 15632, U.S.A.

* Corresponding author. E-mail: jryang@ntu.edu.tw

Keywords: AA7050 (Al-Zn-Mg-Cu) aluminum alloy, precipitation,

The overaging heat treatments of welding would greatly affect the change of grain structures, resulting the limitation of the application in the AA7050 (Al-Zn-Mg-Cu) aluminum alloy [1]. The fusion zones and/or heat affected zones would deteriorate the boundary sliding or boundary cracking. In addition, the particle-free zones and the controlled formation and distribution of precipitates such as η_1, η_2 or η_4 [2] near the grain-boundaries would be concerned with the properties of welding. In the present study, we focused on the determine precipitates between two grains employed by Cs-corrected high angle annular dark field scanning transmission electron microscopy (Cs-corrected HAADF-STEM) and established the possible relationship between the identification of precipitates

References
[1] H.L. Wei, et al., Acta Mater. 126 (2017) 413-425.
[2] T.-F. Chung, et al., Acta Mater. 149 (2018) 377-387.

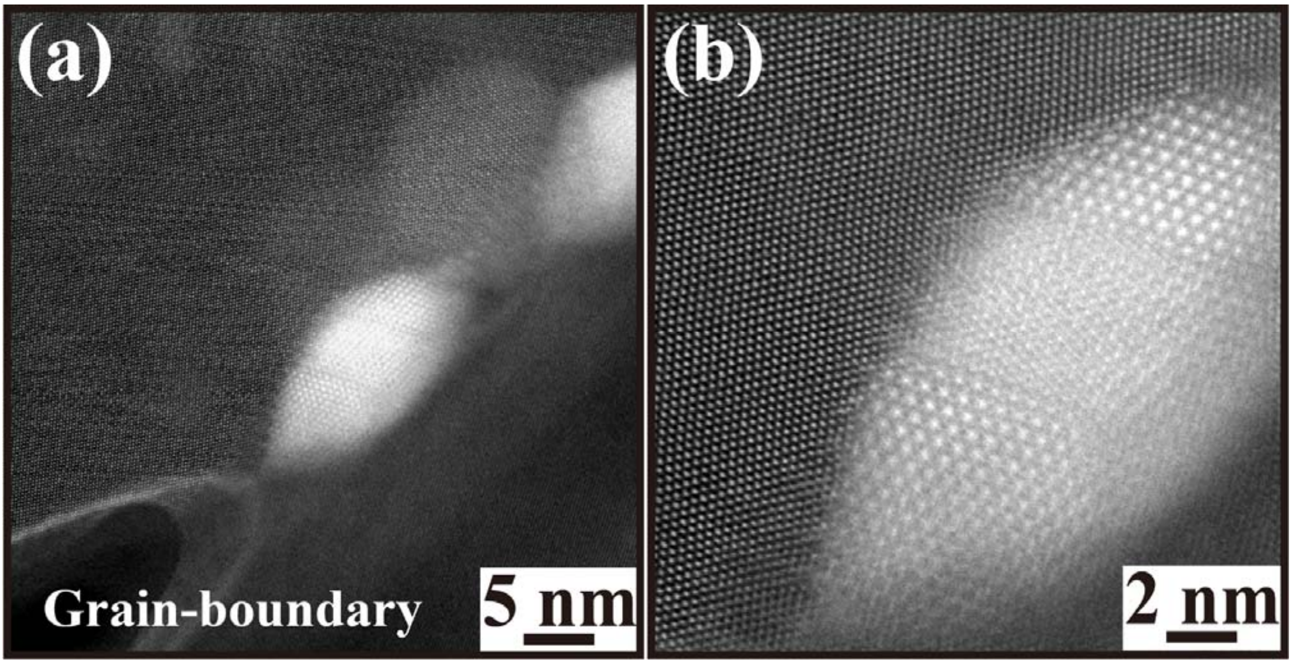

[P07] Investigate the Microstructure Evolution of Cu and In for Low-Temperature Process Application

Yi-Wen Wang[1], H. T. Hung[1], Y. S. Chiu[1], C. R. Kao[1,2,*]

[1] Department of Materials Science and Engineering, National Taiwan University, Taipei, Taiwan
[2] Advanced Research Center of Green Materials Science and Technology, National Taiwan University, Taipei, Taiwan

* Corresponding author E-mail: crkao@ntu.edu.tw

Process temperature is one of the most critical parameter. High temperature accompanies the chip warpage, component damage and substrate deformation et al. The properites of solder decide the process temperature. In this study, we choose the In-based solder instead of Sn-based solder so that we can successfully reduce the process temperature to 70°C. Although the price of indium is expensive, the solder volume of a micro joint is three orders of magnitudes smaller than a flip chip joint. A small amount of solder is used in micro joints. Therefore, the expensive Indium could be applied in 3D IC package.

The experimental structures are microsystem Cu/In, Ni/In and Cu/In/Ni. The objectives of this study are to observe the intermetallic compounds evolution and the joint reliability at the early, middle and final stage. We found that $CuIn_2$ stably formed and transformed to $Cu_{11}In_9$ slowly at 100°C. It is important to study the rare $CuIn_2$ intermetallic compound because of its unknown temperature stability.

Keywords: In-based solder; 3D IC; $CuIn_2$

[P08] A Cu-Cu Bonding Method Using Preoxidized Cu Microparticles under Formic Acid Atmosphere

Runhua Gao[1, 2*], Jiahui Li [1, 2], Yu-An Shen [2], Hiroshi Nishikawa [1]

[1] Joining and Welding Research Institute (JWRI), Osaka University, Osaka, Japan
[2] Graduate School of Engineering, Osaka University, , Osaka, Japan

* Corresponding author. E-mail: gao594730085@gmail.com

Keywords: Cu-Cu bonding, Cu microparticles, Formic acid, Power device.

Many power semiconductor devices now require high tolerance of current density and reliability at high temperature, therefore Cu-Cu bonding, as a replacement of solder, has raised the level of concerns for its great thermal stability and conductivity. In this study, a low-pressure bonding process was developed to achieve Cu-Cu bonding by sintering the preoxidized Cu microparticles under formic acid atmosphere. Cu microparticles were peroxidized to modified surface and generate a Cu oxide nanostructure, which were then reduced and sintered at 300°C under formic acid atmosphere to obtain the bonding. Shear strength of the Cu-Cu bonding was tested to optimize the parameters of bonding process. Fracture surfaces of the Cu-Cu bonding, as well as cross-sectional microstructures, were observed by scanning electrical microscope (SEM), and the components was identified by X-ray diffraction (XRD). The findings reveal that the process of this Cu-Cu bonding is a promising candidate for satisfying the requirements of power device packaging.

[P09] Synthesis and Electric Conductivity of Ceria-based Electrolyte for Solid Oxide Fuel Cell

Yang, Ting-Yi[1], Wei, Wen-Cheng J.[1]*

[1] Institute of Materials Science and Engineering, National Taiwan University, Taiwan, ROC

* Corresponding author. E-mail: wjwei@ntu.edu.tw

Keywords: solid oxide fuel cell, CeO_2, aging treatment, microstructure, electrical properties.

Ceria-based electrolyte materials are syntheisized by a EDTA-citric acid method. Two samples, $Ce_{0.9}Sm_{0.1}O_2$ (ST00) and $Ce_{0.9}Sm_{0.09}Fe_{0.005}Mn_{0.005}O_2$ (S9HH) are prepared and sintered to single cubic fluorite structure and still kept a solution limit. The microstructure and electrical properties are analyzed, showing S9HH having 96% theoretical density (T.D.) after sintered at 1250 °C for 5 hr, and suitable for an electrolyte of soild oxide fuel cell. Bulk electrical conductivity of S9HH is a liner relationship to the reverse of the temperature (1/T). The bulk electrical conductivity of S9HH samples is $7.15*10^{-2}$ $S{\cdot}cm^{-1}$ higher than that of ST00 samples $2.60*10^{-2}$ $S{\cdot}cm^{-1}$ at 800°C. Both of the activated energy of ceria-based materials are around 1.10-1.20 eV, indicating the same conductivity mechanism by oxygen vancacy/ion exchange. A poor electrical performance of ST00 sample is namely due to grain boundary resistance obseverd by impendance and TEM analysis. After an aging treatment at 650 °C for a holding time of 500 h, the electrical conductivity of S9HH is $3.11*10^{-2}$ $S{\cdot}cm^{-1}$ still higher than that of ST00 $1.60*10^{-2}$ $S{\cdot}cm^{-1}$ at 800 °C. Therefore, S9HH is chosen as the electrolyte in solid oxide fuel cells for further investigations.

[P10] Influence of atmosphere on the interfaces of aluminum nitride brazed with graphite paper

Tsung-Te Chou*, Wei-Hsing Tuan

Department of Materials Science and Engineering, National Taiwan University, Taipei, 106, Taiwan

* Corresponding author. E-mail: b99507035@ntu.edu.tw

Keywords: joining, brazing, interface, ceramic, atmosphere

Graphite paper is a material exhibits good conductivity along its surface because of its highly ordered structure. However, the weak bonds between its planes lead to low strength and thus limits its application. As the result, a ceramic plate can be used as a backing layer to support the structure. In this study, graphite paper was joined with aluminum nitride by active brazing alloy Ticusil (68.8%Ag-26.7%Cu-4.5%Ti)

Most of the brazing process were conducted under vacuum or inert gas atmosphere such as nitrogen or argon. In this study, 5% H_2 – 95 % N_2 gas and argon were chosen as brazing atmosphere. Specimen joined under vacuum was also prepared to compare the influence of atmosphere. Morphology of interfaces, composition of reaction products at interface are then analyzed.

The brazing of aluminum nitride and graphite paper can be successfully conducted with Ticusil as braze foil, holding at 1050 °C for 15 min in 5% H_2 – 95 % N_2 gas and argon atmosphere. The brazing under vacuum was conducted at 900 °C. During the joining process, the active element Ti would form reaction products on both AlN-Ticusil interface and graphite-Ticusil. The reaction phase at the AlN-Ticusil interface consists of TiN and Ti-Cu-Al-N intermetallic compounds, while at the graphite-Ticusil interface is mainly composed of TiC. The morphology of the reaction products at AlN-Ticusil interface was also changed from column structure to dispersed particles when joined under vacuum and in nitrogen-rich or argon atmosphere, respectively.

[P11] Effect of Alloying Elements on Corrosion Resistance of Austenitic Stainless Steel

Y. Kanno[1]*, S. Tokita[2], K. Kadoi[2], H. Inoue[2]

[1] Graduate School of Engineering, Osaka University, Osaka, Japan
[2] Joining and Welding Research Institute (JWRI), Osaka University, Osaka, Japan

* Corresponding author. E-mail: y-kanno@jwri.osaka-u.ac.jp

Keywords: stainless steel, EPR test, Pitting potential measurement

The performance and life of a structure are often influenced by that of welds. deterioration of corrosion resistance in welds has been an important problem depending on its operating environment, even in stainless steel which is known to have excellent corrosion resistance. Many researched have been done in the corrosion of weld heat affected zones such as weld decay. However, there are few reports focusing on pitting corrosion and intergranular corrosion of weld metal. In addition, as alloying elements of weld metal changes, the microstructure changes greatly due to segregation, the formation of the secondary phase and coarsening of the columnar grains. Therefore, the aim of this work to examine the corrosion resistance and the microstructure of austenitic stainless steel weld metal with various chemical compositions, in order to improve the characteristics and reliability.

Type 304 and 347 austenitic stainless steels base material and various filler wires are used to prepare weld metal with varying contents of Cr, Ni, Mo, and Nb. In order to evaluate corrosion resistance, reactivation rate and pitting corrosion potential were measured by electrochemical potentiokinetic reactivation (EPR) test and pitting potential measurement, respectively. The reactivation rate of the specimen with high Cr and Mo content was remarkably low. In the pitting potential measurement, specimens with the higher pitting index tend to show higher pitting potential. In order to investigate the concentration of alloying elements, area analysis by EPMA was performed. Cr and Mo were segregated at the dendrite cell boundaries. Thus, it was considered that segregation of Cr and Mo affect corrosion resistance. The analysis of the secondary phase as the origins of pitting corrosion was carried out by EDX analysis. The pitting corrosion initiated along the secondary phases which contained Nb. It was suggested that the secondary phase led to the initiation of pitting corrosion.

[P11] A Cu-Cu Bonding Method Using Preoxidized Cu Microparticles under Formic Acid Atmosphere

Runhua Gao[1, 2]*, Jiahui Li [1, 2], Yu-An Shen [2], Hiroshi Nishikawa [1]

[1] Joining and Welding Research Institute (JWRI), Osaka University, Osaka, Japan
[2] Graduate School of Engineering, Osaka University, , Osaka, Japan

* Corresponding author. E-mail: gao594730085@gmail.com

Keywords: Cu-Cu bonding, Cu microparticles, Formic acid, Power device.

Many power semiconductor devices now require high tolerance of current density and reliability at high temperature, therefore Cu-Cu bonding, as a replacement of solder, has raised the level of concerns for its great thermal stability and conductivity. In this study, a low-pressure bonding process was developed to achieve Cu-Cu bonding by sintering the preoxidized Cu microparticles under formic acid atmosphere. Cu microparticles were peroxidized to modified surface and generate a Cu oxide nanostructure, which were then reduced and sintered at 300°C under formic acid atmosphere to obtain the bonding. Shear strength of the Cu-Cu bonding was tested to optimize the parameters of bonding process. Fracture surfaces of the Cu-Cu bonding, as well as cross-sectional microstructures, were observed by scanning electrical microscope (SEM), and the components was identified by X-ray diffraction (XRD). The findings reveal that the process of this Cu-Cu bonding is a promising candidate for satisfying the requirements of power device packaging.

[P12] Application of electroless Ni and Cu plating for chip-to-chip direct bonding

Li-Yu Kao[1], C. Y. Yang[2], H. T. Hung[3], C. R. Kao[4]*

Department of Materials Science and Engineering, National Taiwan University, Taiwan

* Corresponding author. E-mail: crkao@ntu.edu.tw

Keywords: electroless plating, bonding, interconnections, high uniformity

Controlled flow electroless Ni and Cu plating are currently able to bond Cu pillars to form interconnections between chips with high uniformity. Electroless process has the advantages of low operating temperature, and presureless requirement. The operating temperature of electroless Ni is around 70 °C, and that of electroless Cu can be as low as 50 °C. In this process, polydimethylsiloxane (PDMS), is used to fabricate microchannel, which when combined with a glass plate forms an airtight fixture. Thereafter, chips are placed inside a fixture through which electroless bath is being pumped by a syringe pump. The bonded chips were debonded and analyzed by scanning electron microscope. The results show that both electroless Ni and Cu plating have the ability to join chip interconnections with high uniformity and without serious extraneous deposition.

[P13] Organic-Inorganic Direct Bonding Utilized in Flexible Electronic Packaging

Tilo H. Yang[1,2*], C. Robert Kao[1], Akitsu Shigetou[2]

[1] Department of Materials Science and Engineering, National Taiwan University, Taipei 10617, TAIWAN
[2] National Institute for Materials Science (NIMS), Tsukuba, JAPAN

* Corresponding author. E-mail: f03527057@ntu.edu.tw

Keywords: Heterogeneous integration, direct bonding, organic-inorganic hybridization, flexible and wearable electronics, human-machine interface.

Organic-inorganic material hybridization at the solid-state level is indispensable for the integration of IoT applications [1], but still remains a challenging issue. Existing bonding strategies in the field of electronic packaging tend to employ vacuum or ultrahigh temperature; however, these can cause process complications and material deterioration. Here we report an easy-to-tune method to achieve hybrid bonding at the solid-state level and under the ambient atmosphere. Vacuum-ultraviolet (VUV)-induced reorganization with ethanol was used to develop hydroxyl-carrying alkyl chains through coordinatively-bonded carboxylate onto aluminum, whereas numerous hydroxyl-carrying alkyls were created on polyimide [2, 3]. The triggering of dehydration through these hydroxyls by merely heating at 150°C for a few of minutes produced robust an aluminum/polyimide interface. The as-bonded aluminum/polyimide interface was experimentally proven to be robust and anti-hydrolytic. In addition, the E-VUV process was applicable to other material combinations like Sn-, SiO_2-, Fe-, Ti-, and PEEK-polyimide. For the first time organic-inorganic bonding at the solid-state level was achieved using the ethanol-assisted VUV (E-VUV) process, a strategy which should be applicable to a diversity of plastics and metals with native oxides.

References
[1] S. Xu et al., Science, 344, 70-74 (2014).
[2] H.W. Yang, C.R. Kao, and A. Shigetou, Langmuir, 33, 8413-8419 (2017).
[3] T.H. Yang, C.R. Kao, and A. Shigetou, Sci. Rep., 9, 504 (2019).

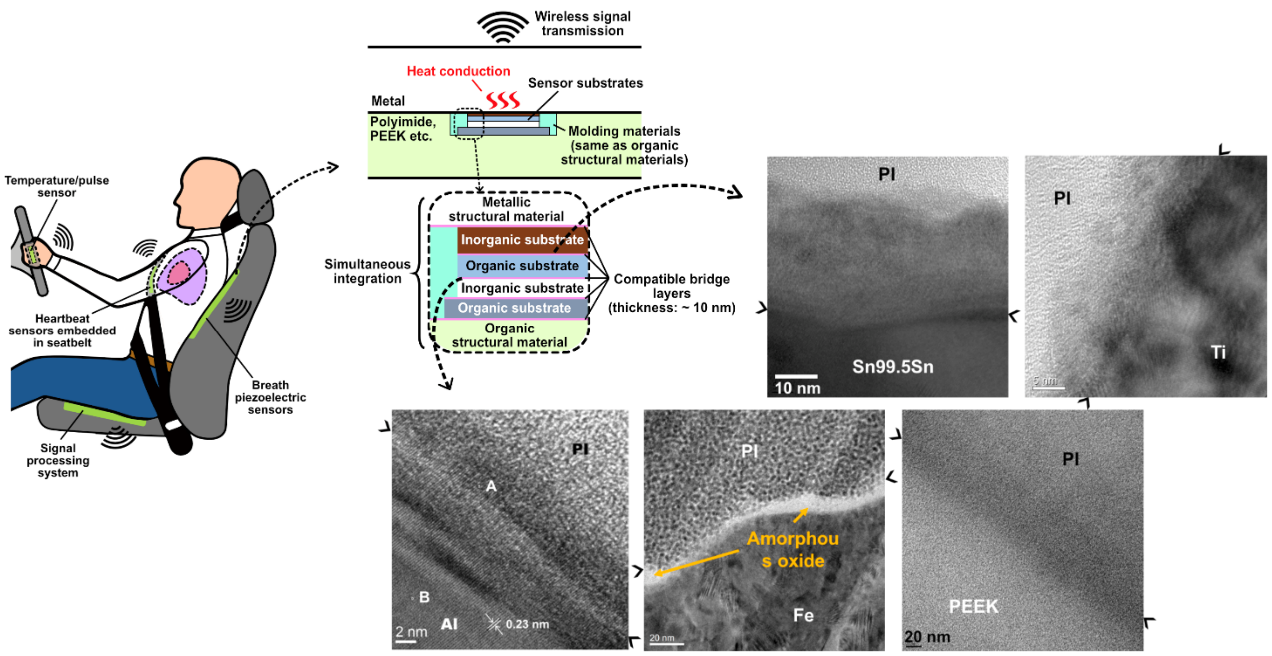

[P14] Comparison on microstructure and tensile properties of nitrogen strengthening in commercially pure titanium (CP-Ti), fabricated by conventional powder metallurgy (PM) and Additive Manufacturing (AM)

A. Issariyapat[1]*, T. Song[2], J. Umeda[3], K. Kondoh[3]

[1]Department of Mechanical Engineering, Graduate School of Engineering, Osaka, Osaka University
[2] School of Aerospace, Mechanical and Manufacturing Engineering, RMIT University, Australia
[3] Joining and Welding Research Institute (JWRI), Osaka University, Osaka, Japan

* Corresponding author. E-mail: ammarueda@jwri.osaka-u.ac.jp

Keywords: commercially pure titanium, powder metallurgy, additive manufacturing, tensile properties

Powder metallurgy (PM) of titanium and titanium alloys is an attractive method in many industries such as automobile, aerospace and medical application [1]. Currently, the PM route has jumped into the new high potential technology as known as additive manufacturing (AM) or 3D printing process. This gains benefit involving freedom three dimensional complicated part of designing, reducing materials buy to weight ratio and save production time, in contrast with the conventional manufacturing methods [2]. In previous studies about the interstitial strengthening such as oxygen (O), nitrogen (N) and carbon (C), shows an advantage to the mechanical properties improvement of titanium materials by solid solution strengthening mechanism [3-4]. Therefore, this work aims to develop titanium with nitrogen solid solution produced by AM process compared to the conventional PM route. The study on microstructure and tensile properties will be presented.

Spark plasma sintering (SPS) and laser engineered net shaping (LENS) were used to consolidate commercially pure Ti with varying nitrogen content in this study. The additional heat treatment on LENSed specimen was also applied on the LENSed Ti-0.5 wt.%N sample to enhance the ductility. Firstly, to attempt to add the nitrogen atom solute into the α-Ti matrix, a tube furnace was employed with heat treatment pure Ti powder in the nitrogen gas atmosphere varying from 913 K to 1013 K for 0.6 ks. Considering the investigation in this work, the effect of nitrogen solute in titanium on tensile properties was analyzed, and microstructure were characterized by electron backscatter diffraction (EBSD), displayed in inverse pole figure (IPF) profile and image quality (IQ). The grain size and morphology were also discussed. According to the microstructure characterization, equiaxed and lamellar structure of as-SPSed sample and fine needle-like phase (α′) were the predominant microstructure found in as-LENSed sample. The improved mechanical properties by increasing nitrogen content showed the strength improvement of both SPSed and LENSed sample. SPSed Ti-0.4 wt.%N specimen revealed UTS of 755 MPa, which was 104 % compared to pure Ti material. The elongation, however, drastically decreased in increasing the nitrogen content, and was almost zero when the nitrogen reached to 0.5 wt.%. On the other hand, the LENSed Ti-0.5 wt.%N specimens indicated higher UTS of 965 MPa compared to the SPSed specimen (approximate 35% improvement) while elongation drastically dropped to 7.6%. HT-LENSed sample showed a small strength decrement to 822 MPa, while its elongation increased to 10.8%. According these results, nitrogen solid solution was effective to obtain a good balance between high tensile strength and enough ductility of LENSed Ti-(N) alloys by combination with heat treatment.

References

[1] Z. Z. Fang et al., Int. Mater. Rev., 63, 407-459 (2018).
[2] D. Herzog, V. Seyda, E. Wycisk, and C. Emmelmann, Acta Mater., 117, 371–392 (2016).
[3] R. I. Jaffee, Progress in Metal Physics, 7, 65-106 (1958)
[4] K. Kondoh et al., Int J Powder Metal, 50, 35-40 (2014).

[P15] Mechanical Properties of FeMnSi-based Medium-Entropy Alloy

Kaifan Lin, S. C. Chen, H. W. Yen, H. C. Lin *,

Department of Materials Science and Engineering, National Taiwan University, Taipei,Taiwan

* Corresponding author. E-mail: hclinntu@ntu.edu.tw

Keywords: high entropy, mechanical property, FeMnSi

As Cantor alloy, equiatomic CoCrFeMnNi, was reported to behave a single crystal with a face-centered cubic (FCC) structure, it has triggered a new era for alloy design and bring the novel concept of high entropy alloy. In this work, vacuum arc melting technique was used to achieve a FeMnSi-based medium entropy alloy (MEA) with 5% Co, 12.5% Cr and 5% Ni (in atomic). Here, after cold rolling, the FeMnSi-based MEA was sliced into the dog-bones shaped tensile specimen. And selected annealing condition have satisfied its full recrystallization. Meanwhile the grain sizes have been controlled under different values.

The results illustrate that the yield strength and tensile strength of FeMnSi-based MEA are stronger than those of CoCrFeMnN HEA. And the microstructure of the tensile specimen coincides with the observation from G. Laplanche et al.[1]. Here, we found intense dislocations and deforming twinning. In summary, the low-cost FeMnSi-based MEA has an FCC crystal structure, and it behaves well ductility and strong strength.

References
[1] G. Laplanche., Acta Mater. 118, 152–163 (2016).

[P16] Interfacial Reactions of Copper with Indium

Han-Tang Hung* and C. Robert Kao

Department of Materials Science and Engineering, National Taiwan University, Taipei, Taiwan

* Corresponding author. E-mail: d05527004@ntu.edu.tw

Keywords: Low-temperature bonding; Solid-liquld interfacial reaction; Indium

Under the rapid development of internet of things (IoT), solid-liquid interdiffusion bonding (SLID) is indispensable for the integration due to its low bonding temperature and high working temperature. Sn-based alloys, such as Sn and SAC(Sn-Ag-Cu), are the most commonly used solders nowadays. Since the melting points of Sn and SAC are 232°C and 217-220°C respectively, the bonding temperature of at least 240°C is required. However, some sensitive devices, such as sensors and flexible biochips, cannot withstand the bonding temperature above 200°C. Therefore, it is essential to develop a new SLID process with lower melting point solder materials so as to reduce the bonding temperature. For pure metals, only the alkali metals and In (T_m=156.76°C) have the melting points between 30°C and 200°C. Nevertheless, since the alkali metals are all soft and highly reactive metals at room temperature and pressure, they only candidate comes out to be In, which is the solder material in this research. Commonly used Cu was chosen as the substrate material. Solid-liquid reaction at 180°C and solid-solid reactions at 100°C, 120°C, and 140°C between In and Cu are investigated in this research. Ar ion milling system with a liquid nitrogen cooling unit (HITACHI IM4000plus) was applied in our research to prevent the difficulty of metallurgical examination. The microstructure evolution was analyzed by scanning electron microscopy (SEM) and energy dispersive X-ray spectroscopy (EDX).

[P17] Injectable and Biodegradable Calcium Sulfate Composite Bone Cement

Pei-Yi Hsu[1]*, Ying-Chen Chen[1], Ting-An Lin[3], Wei-Hsing Tuan[1], Po-Liang Lai[2], Li-Kuan Chang[3]

[1] Department of Materials Science & Engineering, National Taiwan University, Taipei, Taiwan
[2] Department of Orthopedic Surgery, Chang Gung Memorial Hospital, Taoyuan, Taiwan
[3] Department of Biochemical Science and Technology, College of Life Science, National Taiwan University, Taipei, Taiwan

* Corresponding author. E-mail: edwina_hsu@mail2000.com.tw

Keywords: calcium sulfate, calcium phosphate, bone cement, injectable, paste

Calcium phosphate bone cement (CPC) was mainly used to be bone repairing materials in clcinc for years, and so that as well as calcium sulfate bone cement (CSC). They all are capable of bioresorbable, setting, osteoconductive, and biocompatible properties. However, their setting products have the lower compressive strength than of PMMA bone cement commonly used in medication. Here is provide a strategy for calcium sulfate hemihydrates, have sensitively happened hydration reaction with water and fast biodegradability in vitro test, to improve and modify the properties of calcium sulfate hemihydrates to mimic bone. Composing the two phases of calcim phospfate and calcium sufates cement powder midxtures with boddgradable biopolymers (e.g. PPF, collagen, PEG, chitosan, agar etc.) or hardening liquid (phosphoric buffered solution). during the cement setting reaction. The developed biocomposite based on calcium sulfates can presented as injectable paste, porous monolithic, and self-setting bone cement in which shape. The investigation of calcium sulfate biocomposites can be characterized and verified by the X-ray diffraction, electron microscopy, optical microscopy, FTIR, viscosity, setting time measurement, thermos-analysis, degradable test, water resistance, and cell cultured etc. The results indicated the biodegradable biocomposites based on calcium sulfates can show the lower biodegradable rate, biocompatibility, bioactive, porous structure, self-setting with hardening liquid and provide for the biomedical applications in orthopedic surgeries, compared to calcium phosphates.

References

[1] S. Shahbazi, Mater. Sci. & Eng. C 69, 1201–1209 (2016).
[2] S. Li, Cera. Int. 44, 16237–16245 (2018).
[3] H. Chen, PhD Thesis 2017, Maastricht University, Maastricht, The Netherlands. ISBN: 978-94-6233-600-1
[4] D. Banoriya, Materials Today: Proceedings 4, 3534–3541 (2017).
[5] Shelley R. Winn, Biomaterials 21, 2413}2425 (2000).

[P18] Edge effect and Ni distribution in Cu-Sn-Ni micro bump

Haiyang Yu, C. Robert Kao*

Department of Materials Science and Engineering, National Taiwan University

* Corresponding author. E-mail: crkao@ntu.edu.tw

Keywords: $(Cu,Ni)_6Sn_5$, surface diffusion, 3D reconstruction, voids rate, reliability

The three-dimensional integrated circuits (3D ICs) technology is a useful way to continue miniaturization of electronics devices, and Cu-Sn-Cu and Cu-Sn-Ni is the most commonly used structures. Recent years, some researchers have reported many results about Cu-Sn-Cu and Cu-Sn-Ni structure in solid-liquid reaction, but there is few of studies about solid-solid condition, especially for the size of micro joint. In this study, the Cu-Sn-Ni micro joint by electroplating is prepared, after different time aging and polishing, scanning electron microscope (SEM), focused ion beam (FIB), and transmission electron microscope (TEM) are used for analysis the sample. From the results, some conclusions like voids distribution, the edge effect due to surface diffusion and special phase in the intermetallic compound（IMC） have been came to.

References

[1] Tu K N, Thompson R D. Kinetics of interfacial reaction in bimetallic Cu Sn thin films[J]. Acta Metallurgica, 1982, 30(5): 947-952.

[2] Tu K N. Interdiffusion and reaction in bimetallic Cu-Sn thin films[J]. Acta Metallurgica, 1973, 21(4): 347-354.

[3] Kao C R. Microstructures developed in solid-liquid reactions: using Cu-Sn reaction, Ni-Bi reaction, and Cu-In reaction as examples[J]. Materials Science and Engineering: A, 1997, 238(1): 196-201.

[4] Wang Y W, Lin Y W, Kao C R. Kirkendall voids formation in the reaction between Ni-doped SnAg lead-free solders and different Cu substrates[J]. Microelectronics Reliability, 2009, 49(3): 248-252.

[5] Nogita K, Nishimura T. Nickel-stabilized hexagonal (Cu, Ni) 6Sn5 in Sn–Cu–Ni lead-free solder alloys[J]. Scripta Materialia, 2008, 59(2): 191-194

[6] Nogita K, Gourlay C M, McDonald S D, et al. Kinetics of the η–η′ transformation in Cu6Sn5[J]. Scripta Materialia, 2011, 65(10): 922-925.

[7] Mo L, Guo C, Zhou Z, et al. Microstructural evolution of Cu–Sn–Ni compounds in full intermetallic micro-joint and in situ micro-bending test[J]. Journal of Materials Science: Materials in Electronics, 2018, 29(14): 11920-11929.

[8] http://www.geocities.jp/sato5fu/L-Vreview.htm